Wide-angle meta-optical projectors

Hung-I Lin[1,2], Luigi Ranno[1], Padraic Burns[2], Fan Yang[1,2], Hanyu Zheng[1,2], Tian Gu[1,2], and Juejun Hu[1,2]

[1]Department of Materials Science and Engineering, Massachusetts Institute of Technology, Cambridge, MA, USA
[2]2Pi Inc., Cambridge, MA, USA

ABSTRACT

Optical projectors constitute the core component for projection display, structured light, and Light Detection and Ranging (LiDAR) modules. In recent years, metasurfaces have become a strong contender for next-generation optical projection engines offering significant benefits in size, weight, and power consumption. The ability for metasurface to bend optical beams at extreme angles further enables wide-angle beam projection useful for emerging applications such as panoramic sensing and immersive displays. Here we report the design and experimental implementation of a metasurface-enabled wide-angle beam projector.

Keywords: Metasurfaces, optical projection, LiDAR, display

1. INTRODUCTION

Wide field-of-view (WFOV) optics, exemplified by fisheye lenses featuring a FOV close to or even exceeding 180˚, are widely employed in landscape photography, security surveillance, meteorology, and image projection. In recent years, they are also starting to gain traction in emerging electronics and optics products, enabling panoramic cameras and 3-D depth sensors, near-eye displays, AR/VR optics rendering immersive experiences, omnidirectional computer vision systems, and new biomedical imaging instruments[1–9]. To fulfill these application demands, suppression of off-axis optical aberrations such as coma, astigmatism and field curvature is crucial to realizing high-quality WFOV optics. The traditional approach for aberration mitigation entails cascading multiple lens elements, which however increases the size, weight, complexity, and cost of the optical system.

Flat optics based on optical metasurfaces or sub-wavelength diffractive optical elements (DOEs) offer an alternative solution to conventional refractive or reflective elements[10–20]. Metasurface-based designs have been widely employed for constructing planar ultra-thin lenses, also called metalenses[21–31], to mitigate several types of aberrations[32], in particular spherical[22] and chromatic[33–36] aberrations. However, angle-dependent aberrations (e.g., coma, astigmatism, and field curvature) are among the major challenges that must be overcome to realize optical systems with enhanced functionalities while maintaining a minimum element count[37–44]. One approach entails engraving metasurfaces on spherical surfaces, which however poses a non-trivial fabrication challenge[32]. Another solution involves cascading multiple metasurfaces based on traditional bulk optical system design principles. In such doublet metalens designs[37,38], the focusing function is primarily performed by one of the metasurfaces while the other acts to correct the off-axis wavefront aberrations. Diffraction-limited FOV up to approximately 56° was demonstrated in such doublets[37]. Combining a single-layer metasurface or diffractive lens with a physical or virtual optical aperture provides an architecturally simpler approach[45–48]. In particular, we demonstrated a metalens design which achieves an unprecedented near-180˚ FOV while maintaining high optical quality[49]. The metalens design comprises a single piece of flat transparent substrate with an input aperture positioned on the front surface and a metasurface positioned on the back surface. The architecture is wavelength-agnostic and can be scaled to other wavelengths (e.g., long-wave infrared[50]) as well.

In this paper, we will leverage the wide-FOV metasurface design to demonstrate a chip-scale platform for efficient coupling from single-mode photonic integrated circuits (PICs) to a large-area, diffraction-limited beam over near-180˚ FOV. The technology can be used to realize a chip-scale LiDAR or projection display with ultrawide FOV and low loss.

*hujuejun@mit.edu; phone 1-302-766-3083

Photonic and Phononic Properties of Engineered Nanostructures XV, edited by
Ali Adibi, Shawn-Yu Lin, Axel Scherer, Proc. of SPIE Vol. 13377, 1337704
© 2025 SPIE · 0277-786X · doi: 10.1117/12.3052225

2. METASURFACE DESIGN AND FABRICATION

The wide-FOV metasurface is designed for operation at 1550 nm wavelength. The meta-atoms are made of a-Si deposited on a glass wafer substrate. We adopt a cylindrical meta-atom design, where the diameters of the meta-atoms are varied. Height of the meta-atom nanopillars is optimized so as to provide optical phase delay ranging from 0 to 2π while maintaining high optical transmission. The optimized meta-atom design is summarized in Fig. 1. The result indicates that we can obtain > 90% transmission across the entire 0 to 2π phase range.

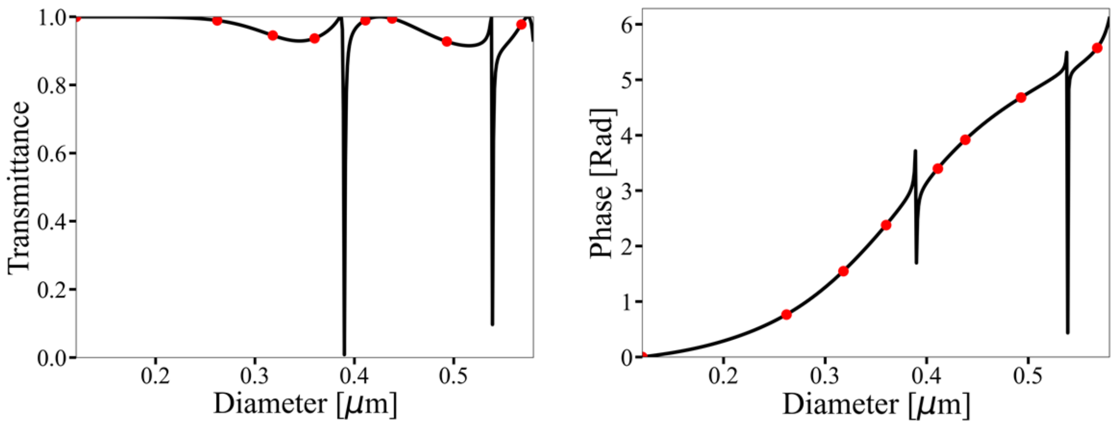

Figure 1. Simulated (left) transmittance and (right) phase of meta-atoms as functions of their diameters. The red dots represent the 8 meta-atom designs used to construct the metalens.

Design of the metasurface follows an analytical procedure we previously developed[51]. The metasurface fabrication process involves plasma enhanced chemical vapor deposition (PECVD) of a-Si on glass wafers, electron beam lithography patterning, plasma etching, and coating of epoxy to encapsulate the metasurface. Details of the fabrication process can be found elsewhere[52,53]. The fabricated metasurface was subsequently boned to an optical aperture piece (fabricated via photolithography on a black photoresist layer on a separate glass wafer) and diced to obtain the singulated metasurfaces. Fig. 2 shows a scanning electron microscopy (SEM) image of the metasurface prior to epoxy coating, showing excellent patterning fidelity free of defects (the most common defect in metasurfaces being collapse of the nanopillars).

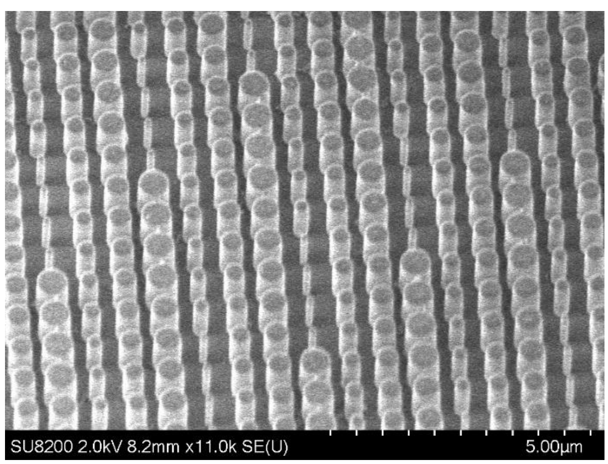

Figure 2. SEM image of a fabricated metasurface prior to encapsulation

3. PIC-METASURFACE INTEGRATION

We further demonstrated wide-angle beam steering using the metasurface coupled with a PIC. The PIC and the metasurface were mounted on two separate 3-axis translational stages to allow relative alignment between them. A test PIC chip fabricated by AIM Photonics[54] containing an array of switchable output ports were used in the demonstration. Laser light from a C-band laser was injected into the PIC through a fiber probe, and routed to different output ports via a series of cascaded on-chip thermo-optic switches. To control the switch arrays, the PIC was wired bonded to a custom printed circuit board (PCB), which connects to a multi-channel source meter such that voltages applied on each switch can be individually set, thereby routing light to different couplers on demand (Fig. 3a). The out-of-plane coupling from the output ports to the metalens used micro-optical reflector arrays (Fig. 3c) fabricated by two photon polymerization[55,56]. The micro-optical reflector couplers offer several key advantages, including small footprint, low coupling loss (> 96%[57]) and broadband operation.

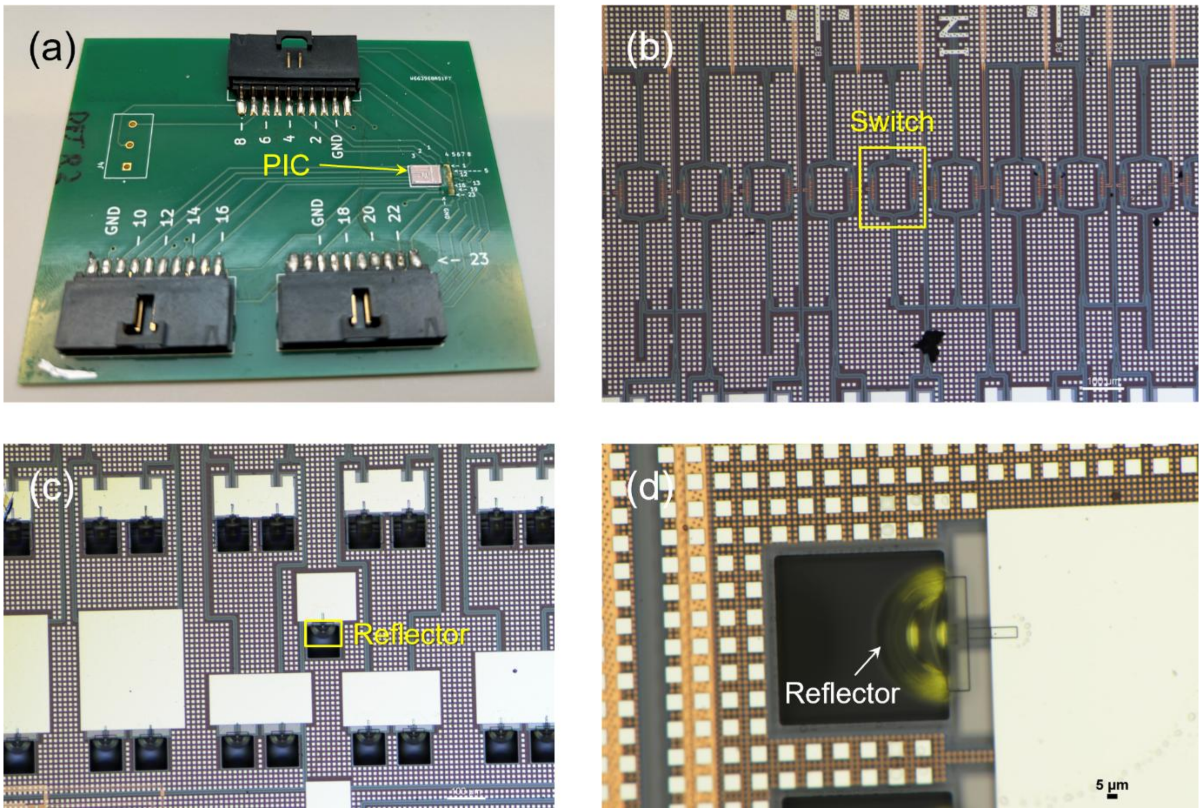

Figure 3. (a) A photo of the PIC mounted on a custom PCB; (b) an optical micrograph of an H-tree structure containing an array of Mach-Zehnder interferometer thermo-optic switches for light routing to the couplers; (c) an optical micrograph showing an array of micro-reflectors for light out coupling to the metalens; (d) enlarged image showing a single micro-reflector printed at the waveguide end facet.

4. WIDE-ANGLE BEAM STEERING DEMONSTRATION

To characterize the steered beam properties exiting from the metasurface at different angles, an optical rail was attached to a custom-made goniometer and aligned to the optical axis of the collimated output beam. The beam steering angle was measured using the goniometer. By capturing the beam cross-sections using a CMOS image sensor mounted on the rail along different positions on the optical axis, the beam size and divergence angle can be quantified. Fig. 4a displays the custom-built measurement setup and Fig. 4b shows the metalens and the PIC aligned to each other during the experiment, noting that the PIC appears blurry as it is 2 mm below the metasurface, a spacing that corresponds to the designed focal length of the metasurface.

Our initial measurement results are summarized in Fig. 5, which plots the beam steering angle as a function of the coupler lateral position. We note that this corresponds to the image height curve of the metalens. Our experimental results (indicated as dots) yield good agreement with the theoretical design (solid line) and demonstrate metalens-assisted beam steering over 120° FOV.

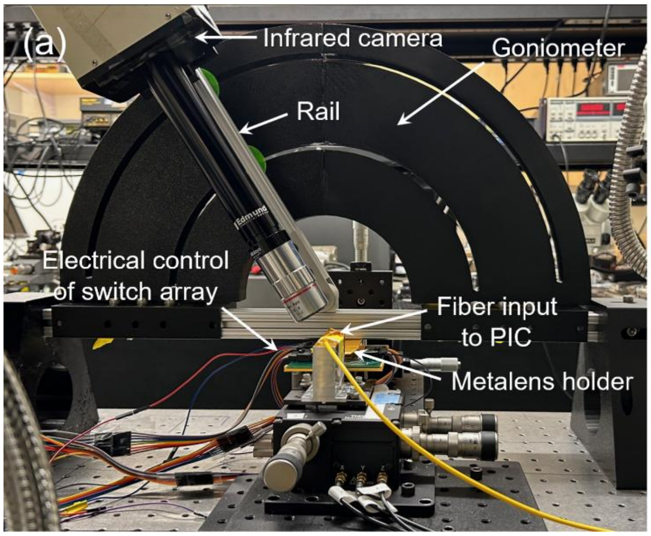

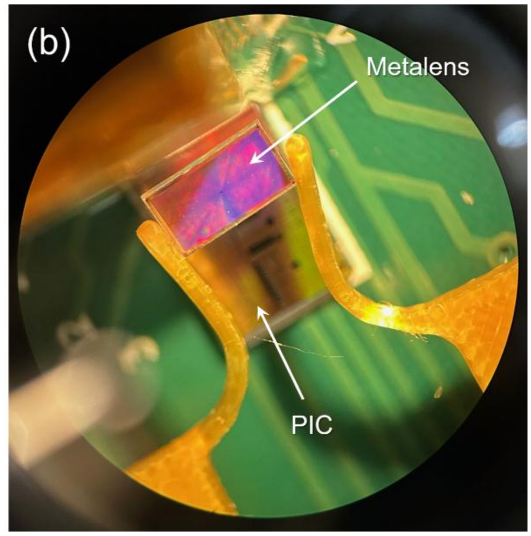

Figure 4. (a) A photo of the PIC-metalens beam steering measurement setup; (b) a photo captured from a microscope showing the metalens positioned on top of the PIC during the beam steering measurement.

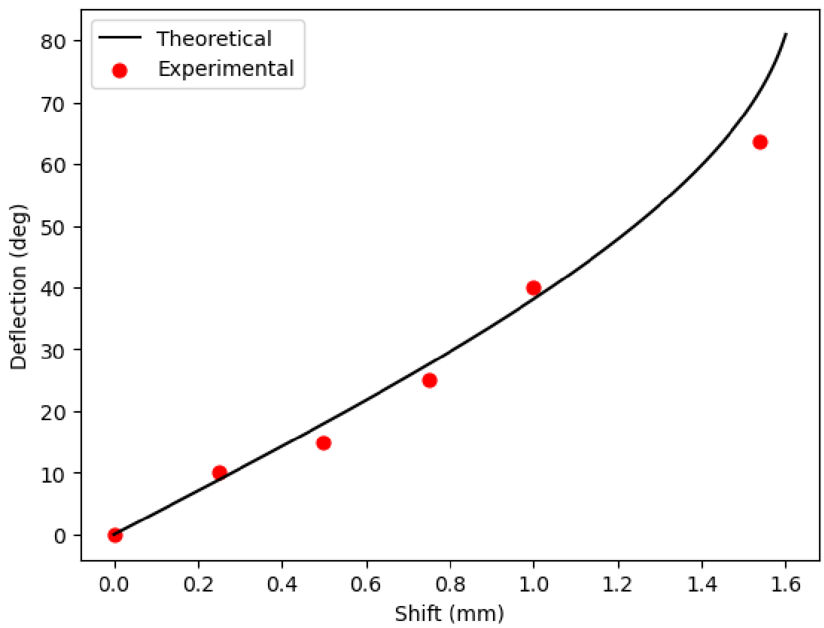

Figure 5. Designed (solid line) and experimentally measured (dots) beam steering angle of the PIC-metalens assembly vs. coupler position on the PIC.

5. SUMMARY

We demonstrated beam steering functionality using a combination of a free-space metasurface coupled to a foundry-processed PIC with switchable on-chip emitter arrays. Metalens-assisted beam steering over 120° FOV was experimentally validated.

REFERENCES

[1] Liu, W., Li, Z., Cheng, H., Tang, C., Li, J., Zhang, S., Chen, S., and Tian, J., "Metasurface Enabled Wide-Angle Fourier Lens," Advanced Materials 30(23), 1706368 (2018).

[2] Jiang, Z.H., Lin, L., Ma, D., Yun, S., Werner, D.H., Liu, Z., and Mayer, T.S., "Broadband and wide field-of-view plasmonic metasurface-enabled waveplates," Scientific Reports 4, 7511 (2014).

[3] Lee, G.Y., Hong, J.Y., Hwang, S.H., Moon, S., Kang, H., Jeon, S., Kim, H., Jeong, J.H., and Lee, B., "Metasurface eyepiece for augmented reality," Nature communications 9(1), 4562 (2018).

[4] Guo, Y., Ma, X., Pu, M., Li, X., Zhao, Z., and Luo, X., "High-Efficiency and Wide-Angle Beam Steering Based on Catenary Optical Fields in Ultrathin Metalens," Advanced Optical Materials 6(19), 1800592 (2018).

[5] Lassalle, E., Mass, T.W.W., Eschimese, D., Baranikov, A. V., Khaidarov, E., Li, S., Paniagua-Dominguez, R., and Kuznetsov, A.I., "Imaging Properties of Large Field-of-View Quadratic Metalenses and Their Applications to Fingerprint Detection," ACS Photonics 8(5), 1457–1468 (2021).

[6] Liu, Y., Yu, Q.Y., Chen, Z.M., Qiu, H.Y., Chen, R., Jiang, S.J., He, X.T., Zhao, F.L., and Dong, J.W., "Meta-objective with sub-micrometer resolution for microendoscopes," Photonics Research 9(2), 106–115 (2021).

[7] Chen, C., Chen, P., Xi, J., Huang, W., Li, K., Liang, L., Shi, F., and Shi, J., "On-chip monolithic wide-angle field-of-view metalens based on quadratic phase profile," AIP Advances 10(11), 115213 (2020).

[8] Ni, Y., Chen, S., Wang, Y., Tan, Q., Xiao, S., and Yang, Y., "Metasurface for Structured Light Projection over 120° Field of View," Nano Letters 20(9), 6719–6724 (2020).

[9] Mirzapourbeinekalaye, B., Mansouree, M., McClung, A., and Arbabi, A., "Fast and wide-angle integrated laser beam scanner enabled by a metalens," in Proc. SPIE PC12432, PC124320Q (2023).

[10] Yu, N., Genevet, P., Kats, M. a, Aieta, F., Tetienne, J.-P., Capasso, F., and Gaburro, Z., "Light Propagation with Phase Discontinuities Reflection and Refraction," Science 334(October), 333–337 (2011).

[11] Ni, X., Emani, N.K., Kildishev, A. V., Boltasseva, A., and Shalaev, V.M., "Broadband Light Bending with Plasmonic Nanoantennas," Science (New York, N.Y.) 335(6067), 427–427 (2012).

[12] Pors, A., and Bozhevolnyi, S.I., "Efficient and broadband quarter-wave plates by gap-plasmon resonators," Optics Express 21(3), 2942–2952 (2013).

[13] Kuznetsov, A.I., Miroshnichenko, A.E., Brongersma, M.L., Kivshar, Y.S., and Luk'yanchuk, B., "Optically resonant dielectric nanostructures," Science (New York, N.Y.) 354(6314), aag2472 (2016).

[14] Capasso, F., "The future and promise of flat optics: A personal perspective," Nanophotonics 7(6), 953–957 (2018).

[15] Achouri, K., and Caloz, C., "Design, concepts, and applications of electromagnetic metasurfaces," Nanophotonics 7(6), 1095–1116 (2018).

[16] Kamali, S.M., Arbabi, E., Arbabi, A., and Faraon, A., "A review of dielectric optical metasurfaces for wavefront control," Nanophotonics 7(6), 1041–1068 (2018).

[17] Campbell, S.D., Sell, D., Jenkins, R.P., Whiting, E.B., Fan, J.A., and Werner, D.H., "Review of numerical optimization techniques for meta-device design [Invited]," Optical Materials Express 9(4), (2019).

[18] Shaltout, A.M., Lagoudakis, K.G., van de Groep, J., Kim, S.J., Vučković, J., Shalaev, V.M., and Brongersma, M.L., "Spatiotemporal light control with frequency-gradient metasurfaces," Science (New York, N.Y.) 365(6451), 374–377 (2019).

[19] Shalaginov, M.Y., Campbell, S.D., An, S., Zhang, Y., Ríos, C., Whiting, E.B., Wu, Y., Kang, L., Zheng, B., et al., "Design for quality: reconfigurable flat optics based on active metasurfaces," Nanophotonics 9(11), 3505–3534 (2020).

[20] Gu, T., Kim, H.J., Rivero-Baleine, C., and Hu, J., "Reconfigurable metasurfaces towards commercial success," Nature Photonics 17(1), 48–58 (2023).

[21] Shi, H., Wang, C., Du, C., Luo, X., Dong, X., and Gao, H., "Beam manipulating by metallic nano-slits with variant widths," Optics Express 13(18), 6815–6820 (2005).

[22] Aieta, F., Genevet, P., Kats, M.A., Yu, N., Blanchard, R., Gaburro, Z., and Capasso, F., "Aberration-free ultrathin flat lenses and axicons at telecom wavelengths based on plasmonic metasurfaces," Nano Letters 12(9), 4932–4936 (2012).

[23] West, P.R., Stewart, J.L., Kildishev, A. V., Shalaev, V.M., Shkunov, V. V., Strohkendl, F., Zakharenkov, Y.A., Dodds, R.K., and Byren, R., "All-dielectric subwavelength metasurface focusing lens," Optics Express 22(21), 26212–26221 (2014).

[24] Khorasaninejad, M., and Capasso, F., "Metalenses: Versatile multifunctional photonic components," Science (New York, N.Y.) 358(6367), eaam8100 (2017).
[25] Lalanne, P., and Chavel, P., "Metalenses at visible wavelengths: past, present, perspectives," Laser & Photonics Reviews 11(3), 1600295 (2017).
[26] Tseng, M.L., Hsiao, H.H., Chu, C.H., Chen, M.K., Sun, G., Liu, A.Q., and Tsai, D.P., "Metalenses: Advances and Applications," Advanced Optical Materials 6(18), 1800554 (2018).
[27] Lin, D., Fan, P., Hasman, E., and Brongersma, M.L., "Dielectric gradient metasurface optical elements," Science (New York, N.Y.) 345(6194), 298–302 (2014).
[28] Lalanne, P., Astilean, S., Chavel, P., Cambril, E., and Launois, H., "Blazed binary subwavelength gratings with efficiencies larger than those of conventional échelette gratings," Optics Letters 23(14), 1081–1083 (1998).
[29] Shalaginov, M.Y., An, S., Zhang, Y., Yang, F., Su, P., Liberman, V., Chou, J.B., Roberts, C.M., Kang, M., et al., "Reconfigurable all-dielectric metalens with diffraction-limited performance," Nature Communications 12, 1225 (2021).
[30] Chang, S., Zhang, L., Duan, Y., Rahman, M.T., Islam, A., and Ni, X., "Achromatic metalenses for full visible spectrum with extended group delay control via dispersion-matched layers," Nature Communications 15, 9627 (2024).
[31] Arbabi, A., and Faraon, A., "Advances in optical metalenses," Nature Photonics 17(1), 16–25 (2022).
[32] Aieta, F., Genevet, P., Kats, M., and Capasso, F., "Aberrations of flat lenses and aplanatic metasurfaces," Optics Express 21(25), 31530–31539 (2013).
[33] Chen, W.T., Zhu, A.Y., Sanjeev, V., Khorasaninejad, M., Shi, Z., Lee, E., and Capasso, F., "A broadband achromatic metalens for focusing and imaging in the visible," Nature Nanotechnology 13(3), 220–226 (2018).
[34] Wang, S., Wu, P.C., Su, V.C., Lai, Y.C., Hung Chu, C., Chen, J.W., Lu, S.H., Chen, J., Xu, B., et al., "Broadband achromatic optical metasurface devices," Nature Communications 8(1), 187 (2017).
[35] Shrestha, S., Overvig, A.C., Lu, M., Stein, A., and Yu, N., "Broadband achromatic dielectric metalenses," Light: Science & Applications 7(1), 85 (2018).
[36] Zhou, Y., Kravchenko, I.I., Wang, H., Nolen, J.R., Gu, G., and Valentine, J., "Multilayer Noninteracting Dielectric Metasurfaces for Multiwavelength Metaoptics," Nano Letters 18(12), 7529–7537 (2018).
[37] Arbabi, A., Arbabi, E., Kamali, S.M., Horie, Y., Han, S., and Faraon, A., "Miniature optical planar camera based on a wide-angle metasurface doublet corrected for monochromatic aberrations," Nature Communications 7, 13682 (2016).
[38] Groever, B., Chen, W.T., and Capasso, F., "Meta-lens doublet in the visible region," Nano Letters 17(8), 4902–4907 (2017).
[39] Martins, A., Li, K., Li, J., Liang, H., Conteduca, D., Borges, B.H. V., Krauss, T.F., and Martins, E.R., "On Metalenses with Arbitrarily Wide Field of View," ACS Photonics 7(8), 2073–2079 (2020).
[40] Tang, D., Liu, J., Chen, L., and Zhang, X., "Achromatic metasurface doublet with a wide incident angle for light focusing," Optics Express 28(8), 12209–12218 (2020).
[41] Pu, M., Luo, X., Ma, X., Li, X., and Guo, Y., "Nanoapertures with ordered rotations: symmetry transformation and wide-angle flat lensing," Optics Express 25(25), 31471–31477 (2017).
[42] Huang, Z., Qin, M., Guo, X., Guo, X., Guo, X., Yang, C., Yang, C., and Li, S., "Achromatic and wide-field metalens in the visible region," Optics Express 29(9), 13542–13551 (2021).
[43] Engelberg, J., Zhou, C., Mazurski, N., Bar-David, J., Kristensen, A., and Levy, U., "Near-IR wide-field-of-view Huygens metalens for outdoor imaging applications," Nanophotonics 9(2), 361–370 (2020).
[44] Lassalle, E., Mass, T.W.W., Eschimese, D., Baranikov, A. V., Khaidarov, E., Li, S., Paniagua-Dominguez, R., and Kuznetsov, A.I., "Imaging Properties of Large Field-of-View Quadratic Metalenses and Their Applications to Fingerprint Detection," ACS Photonics 8(5), 1457–1468 (2021).
[45] Buralli, D.A., and Morris, G.M., "Design of a wide field diffractive landscape lens," Applied Optics 28(18), 3950–3959 (1989).
[46] Yang, F., Shalaginov, M.Y., Lin, H.I., An, S., Agarwal, A., Zhang, H., Rivero-Baleine, C., Gu, T., and Hu, J., "Wide field-of-view metalens: a tutorial," Advanced Photonics 5(3), 033001 (2023).
[47] Yang, F., An, S., Shalaginov, M.Y., Zhang, H., Rivero-Baleine, C., Hu, J., and Gu, T., "Design of broadband and wide-field-of-view metalenses," Optics Letters 46(22), 5735 (2021).
[48] Yang, F., An, S., Shalaginov, M.Y., Zhang, H., Hu, J., and Gu, T., "Understanding wide field-of-view flat lenses: an analytical solution [Invited]," Chinese Optics Letters 21, 023601 (2023).

[49] Shalaginov, M.Y., An, S., Yang, F., Su, P., Lyzwa, D., Agarwal, A.M., Zhang, H., Hu, J., and Gu, T., "Single-Element Diffraction-Limited Fisheye Metalens," Nano Letters 20(10), 7429–7437 (2020).

[50] Lin, H.I., Geldmeier, J., Baleine, E., Yang, F., An, S., Pan, Y., Rivero-Baleine, C., Gu, T., and Hu, J., "Wide-Field-of-View, Large-Area Long-Wave Infrared Silicon Metalenses," ACS Photonics 11(5), 1943–1949 (2024).

[51] Yang, F., Gu, T., and Hu, J., "Analytical design framework for metasurface projection optics," JOSA B 40(8), 2211–2220 (2023).

[52] Yang, F., Lin, H.-I., Shalaginov, M.Y., Stoll, K., An, S., Rivero-Baleine, C., Kang, M., Agarwal, A., Richardson, K., et al., "Reconfigurable parfocal zoom metalens," Advanced Optical Materials 10, 2200721 (2022).

[53] Yang, F., Lin, H.I., Chen, P., Hu, J., and Gu, T., "Monocular depth sensing using metalens," Nanophotonics 12(14), 2987–2996 (2023).

[54] Fahrenkopf, N.M., McDonough, C., Leake, G.L., Su, Z., Timurdogan, E., and Coolbaugh, D.D., "The AIM Photonics MPW: A Highly Accessible Cutting Edge Technology for Rapid Prototyping of Photonic Integrated Circuits," IEEE Journal of Selected Topics in Quantum Electronics 25(5), 8201406 (2019).

[55] Ranno, L., Sia, J.X.B., Popescu, C., Weninger, D., Serna, S., Yu, S., Kimerling, L.C., Agarwal, A., Gu, T., et al., "Highly efficient fiber to Si waveguide free-form coupler for foundry-scale silicon photonics," Photonics Research 12(5), 1055–1066 (2024).

[56] Yu, S., Ranno, L., Du, Q., Serna, S., McDonough, C., Fahrenkopf, N., Gu, T., and Hu, J., "Free-Form Micro-Optics Enabling Ultra-Broadband Low-Loss Off-Chip Coupling," Laser & Photonics Reviews 17, 2200025 (2023).

[57] Yu, S., Lu, J., Ginis, V., Kheifets, S., Lim, S.W.D., Qiu, M., Gu, T., Hu, J., and Capasso, F., "On-chip optical tweezers based on freeform optics," Optica 8(3), 409–414 (2021).